Density Functional Study of the Proton Transfer Effect on Vibrations of Strong (Short) Intermolecular O−H···N/O$^-$···H−N$^+$ Hydrogen Bonds in Aprotic Solvents

Shushu Kong,[†] Ilja G. Shenderovich,[†,‡] and Mikhail V. Vener*[,§]

Institut für Chemie und Biochemie, Freie Universität Berlin, Takustrasse 3, D-14195 Berlin, Germany, Department of Physics, St. Petersburg State University, 198504 St. Petersburg, Russia, and Department of Quantum Chemistry, Mendeleev University of Chemical Technology, Miusskaya Square 9, 125047 Moscow, Russia

Received: December 10, 2009; Revised Manuscript Received: January 9, 2010

The structure and spectroscopic properties of the 1:1 complexes of substituted pyridines with benzoic acid and phenol derivatives in aprotic solvents are studied using B3LYP functional combined with the polarizable continuum model approximation. Two extreme structures are investigated: the state without (HB) and with proton transfer (PT). In the presence of an external electric field the O···N distance is contracted and the PT state does appear. The PT state of both the pyridine−benzoic and the pyridine−phenol complexes displays the only IR-active band in the 2800−1800 frequency region, which is located around 2000 cm^{-1}. However, the nature of the band is different for these two complexes. In the pyridine−benzoic acid complex it is practically a pure stretching vibration of the HN$^+$ group, while in the pyridine−phenol complex it is the mixed vibration of the bridging proton. A specific feature of the PT state in the pyridine−phenol complex is an IR-intensive band near 600 cm^{-1}, associated with the asymmetric stretching vibrations of the O$^-$···HN$^+$ fragment. Its intensity is reciprocally proportional to the O···N distance. The appearance of this band provides an efficient criterion to differentiate between the HB and PT states of the 1:1 complexes of phenols with pyridines in aprotic solvents.

Introduction

The present study deals with strong (short) intermolecular O−H···N bonds in the 1:1 hydrogen bonded complexes formed by benzoic acids and phenols with pyridines. In the gas phase the bridging (shared) proton is always located near oxygen and the only state without proton transfer (HB state) exists.[1,2] In the condensed phase the bridging proton shifts along the hydrogen bond (H-bond) toward the base.[3−6] In the extreme case the proton transfer state (PT state) is formed.[7−10] This state is characterized by a large value of the dipole moment[11] and can exist only by being stabilized by an external electric field or a system of coupled H-bonds. Thus, the PT state can appear as a local or the global minimum on the potential (free) energy surface only as a result of the environmental effect. This trend is the same for any system with a moderately strong H-bond. Because of that, the detection of the PT state acquires, besides an academic interest, an important practical application as a tool feasible to inspect the local structure of amorphous materials[12−14] and solid forms of active pharmaceutical ingredients.[15] Vibrational spectroscopy is a powerful experimental method feasible to inspect different types of H-bonds in the gas phase and condensed matter. The frequency and intensity of IR transitions attributed to the OH stretching vibration are used in numerical correlation to estimate geometry,[16] energy[17] and other features of the HB state.[18,19] The situation is different for the PT state. Only a limited number of compounds with the O$^-$···H−N$^+$ fragment were described in detail.[7,10,19−22] The reason is that this fragment does not exist in the gas phase[1,2] and often cannot be identified in solution.[8,23] Thus, it is of significant interest to inspect the spectroscopic properties of the PT state for different 1:1 complexes with a strong (short) intermolecular H-bond.

Adducts of benzoic acids and phenols with pyridines are probably the most studied types of complexes with the O−H···N fragment in solvents and molecular crystals. The complexes of benzoic acids with pyridines are popular building blocks in crystal engineering[24−26] and play an important role in biological systems,[27] including enzymatic centers.[28,29] Although the formation of the PT state can be followed using the asymmetric stretching vibrations of the CO_2^- group,[30] the corresponded frequency is not sensitive to the H-bond strength. The complexes of phenols with pyridines often exhibit proton transfer in crystals if the phenol contains chlorine atoms in the ortho positions.[7,10,19,20,23,31] However, the geometry of the PT state can be hardly characterized by IR spectroscopy, since in some phenol−pyridine complexes the IR-active band in the 2800−1800 frequency region disappears completely.[32]

The overall aim of this study is to overcome these problems and to inspect the spectroscopic properties of the PT state in the considered 1:1 complexes theoretically. The effect of the external electric field on the geometry of the H-bond is taking into account using the polarizable continuum model (PCM) approximation.[33] For these purposes it is necessary (i) to identify the PT state as a local or the global minimum on the potential (free) energy surface and (ii) to investigate the effect of proton transfer on the frequency and IR/Raman intensity of the bridging proton vibrations. Besides that we aim to clarify the specific role of the chlorine atoms in the ortho position of phenol ring for proton transfer in the 1:1 complexes of substituted pyridines with phenol derivatives. For these purposes Bader analysis of the electron density is applied.

Complexes (1:1) of 3-methylpyridine with 2,6-dichloro-4-nitrophenol (Py−Ph) and 2,4,6-trimethylpyridine with 3,5-

[†] Freie Universität Berlin.
[‡] St. Petersburg State University.
[§] Mendeleev University of Chemical Technology.

10.1021/jp911694r
Published on Web 01/27/2010

TABLE 1: Energies of Intermolecular H-Bond and Noncovalent Interactions[a] of Complexes of 3-Methylpyridine (Py) with Substituted Phenols at $\varepsilon = 1$ (Gas Phase)

	H-bond			noncovalent interaction	
complex	R(H···N), Å	E_{int},[b] kJ/mol	$-\Delta H$,[c] kJ/mol	R(H···A),[d] Å	E_{int}, kJ/mol
Py−4-nitrophenol	1.767	41.0	33.0	2.832	4.3
Py−3,5-dichloro-4-nitrophenol	1.740	44.5	55.0	2.797	4.6
Py−2,6-dichloro-4-nitrophenol (Py-Ph)	1.715	48.3	58.5	3.080	2.9

[a] See Figure S1 (Supporting Information). [b] Evaluated using eq 1. [c] Evaluated using eq 2. [d] A = N or Cl, see Figure S1 (Supporting Information).

dinitrobenzoic acid (Py−BZA) are used as the model systems to study the effect of proton transfer on vibrations of short intermolecular O−H···N/O$^-$···H−N$^+$ hydrogen bonds in aprotic solvents. Their structure and IR spectra were studied in the condensed phase where proton transfer was observed.[7,9,23,30] Besides that, they are probably the smallest O−H···N complexes of these types for which proton transfer does occur in the PCM approximation. The strength of the external electric field is proportional to the dielectric permittivity of the media, ε, which has been varied from 2.4 (toluene) to 36.6 (acetonitrile).

Since only the equilibrium solvation is considered, a detailed analysis of the proton transfer free energy surface, and, in particular, an estimation of the potential barrier between the HB and PT states is beyond the scope of the present study.

Computational Methods

B3LYP is the most popular DFT functional,[34] which gives reasonable results for H-bonded complexes.[35] The 6-31G** basis set is used due to the following reasons: (i) it provides reliable results for the structure and properties of H-bonds of different strengths in different phases, including the molecular crystals,[36−40] and (ii) it enables one to perform a direct comparison of the structure and spectroscopic features of H-bonded complexes computed in the condensed phase with those in the gas phase.[41] The use of the double harmonic approximation[42] allows one to obtain a quantitative or semiqualitative description of the frequencies and IR/Raman intensities of the HB and PT states of the 1:1 complexes with the strong H-bond.[43−47] This is why the 6-31G** basis set seems to be sufficient. Indeed, the data collected in Table 2 show that the use of the 6-311++G** basis results in small changes of the geometrical parameters and the OH stretching frequency of the considered complexes in the gas phase.

The structure and IR spectra of the H-bonded complexes in the gas phase and aprotic solvents are computed using Gaussian03[48] with the SCF = Tight option. An effect of aprotic solvent is taken into account in terms of the CPCM approach[49] with the radii = UAHF option. The minimum-energy states of the complexes have been confirmed by calculating the harmonic frequencies.

For the gas phase complexes the topological electron-density properties[50] are evaluated with the AIM2000 computer program suite.[51,52] The following electron-density features at the H···X (X = O, N, Cl) intermolecular bond critical point are considered: (i) the values of the electron density, ρ_b, and (ii) the potential energy density, V_b. The latter is proportional to the energy of the particular noncovalent interaction, E_{int}[53−55] (in atomic units):

$$E_{int} = (1/2)V_b \quad (1)$$

The description of the electron-density topology (the Bader) analysis may be found elsewhere.[56,57]

For comparison, we also estimated the enthalpy of intermolecular H-bonds ($-\Delta H$) by the empirical formulas of Iogansen:[17]

$$-\Delta H = 12.2\Delta I^{1/2} \quad (2)$$

Here ΔH is given in kJ/mol and IR intensities are given in 10^{-2} kM/mol. $\Delta I^{1/2} = I^{1/2} - I_0^{1/2}$, where I and I_0 are the computed values of the IR intensity of the OH stretching vibration in H-bonded complexes and free acids, respectively.

Results

H-Bonding of Ortho-Chloro-Substituted Phenols. To clarify the specific role of Cl in the ortho positions of phenol ring, 1:1 complexes of 3-methylpyridine with chloro-substituted-4-nitrophenols are considered. Since the effect of the ortho-chloro-substitution on H-bonding of phenols is not the main interest of this work, the corresponding numerical values are given in the Supporting Information to this paper, Tables S1 and S2 and Figure S1. Compared are the geometries and the harmonic frequencies of the OH stretching vibration of H-bonded complexes of 3-methylpyridine with 4-nitrophenol, 3,5-dichloro-4-nitrophenol, and 2,6-dichloro-4-nitrophenol (the Py−Ph complex). Both the O···N distance and OH stretching frequency are found to be affected upon the chlorine substitution. The energies of the intermolecular H-bond evaluated using eqs 1 and 2 are given in Table 1. Both approaches lead to similar results; the relative difference is about 20%.

The Bader analysis enables us to detect noncovalent intermolecular interactions in addition to the intermolecular H-bond in these complexes. They are N···H−C(2) interactions in the case of 4-nitrophenol and 3,5-dichloro-4-nitrophenol, Figure S1a (Supporting Information), and a Cl···H−C(2) interaction for 2,6-dichloro-4-nitrophenol, Figure S1b (Supporting Information). The energies of these interactions are about 1 order of magnitude smaller than that of the intermolecular H-bond (4 and 45 kJ/mol, respectively, Table 1). However, they seem to be sufficient to affect the directionality of the H-bond. Specifically the Cl···H−C(2) contact affects strongly the dihedral angle between the pyridine and phenol aromatic rings in the Py−Ph complex, which results in a reduction of the O···N distance, Table S1 (Supporting Information). As a result, proton transfer can occur in the ortho-chloro-substituted phenol−pyridine complexes.[7,10,19,20,23,31] It should be noted that the existence of the intermolecular noncovalent interactions in the Py−Ph molecular crystal was suggested by Sobczyk et al. on the basis of a geometrical criteria.[7]

In the Py−BZA complex the Bader analysis of the electron density reveals a noncovalent intermolecular interaction between the C=O group of 3,5-dinitrobenzoic acid and a methyl group proton of 2,4,6-trimethylpyridine. The energy of this interaction is ~10 kJ/mol.

Structure and Vibrational Spectra of the HB State. In the gas phase approximation, $\varepsilon = 1$, for both complexes, Py−Ph

TABLE 2: Values of Selected Geometrical Parameters and the Harmonic Frequency of the OH Stretching Vibration, ν(OH), of the Py−Ph and Py−BZA Complexes Computed Using the B3LYP/6-31G Approximation at $\varepsilon = 1$[a] (Gas Phase) and at $\varepsilon = 4.9$ (Chloroform)**

	Py−Ph			Py−BZA		
		chloroform			chloroform	
distance (Å)/frequency (cm^{-1})	gas phase	HB state	PT state	gas phase	HB state	PT state
O−H	1.010 (1.006)	1.028	1.369	1.035 (1.032)	1.050	1.449
H···N	1.715 (1.737)	1.628	1.141	1.618 (1.637)	1.568	1.118
O···N	2.648 (2.676)	2.612	2.486	2.647 (2.663)	2.613	2.562
C−O	1.322 (1.322)	1.317	1.278	1.323 (1.322)	1.318	1.282
C═O				1.222 (1.214)	1.224	1.243
C_2−N	1.341 (1.339)	1.342	1.344	1.347 (1.346)	1.348	1.355
C_6−N	1.338 (1.336)	1.340	1.341	1.348 (1.346)	1.349	1.352
ν(OH)	2986 (3005)	2648		2546 (2556)	2289	

[a] For comparison, in parentheses are given values computed using the B3LYP/6-311++G** approximation.

TABLE 3: Harmonic Frequencies (Freq, cm^{-1}), IR Intensities[a] (I, kM/mol), and Raman Scattering Activities (R, A^4/amu) of Vibrations Involving Large Displacements of the Bridging Proton Computed for the HB and the PT States of the Py−Ph Complex at $\varepsilon = 4.9$ (Chloroform)

HB state		PT state	
freq (I, R)[b]	assignment[c]	freq (I, R)	assignment
2648 (5606, 2056)	ν(OH)	1767 (1343, 18)	ν_1[d]
1584 (313, 28)	$\nu_{AS}(NO_2) + \delta$(ring) + δ(OH)	1621 (144, 79)	$\delta(HN^+) + \delta(CH)_{PY} + \delta_S(CH)$
1386 (348, 839)	δ(OH) + ν(CN)	1441 (457, 130)	ν(OHN) + $\delta(CH)_{PY} + \delta_S(CH_3)$
1363 (631, 309)	ν_{AS}(CCC) + δ(OH)	1339 (586, 94)	$\gamma(HN^+) + \nu(ring)_{PY} + \delta(CH)_{PY}$
1349 (243, 107)	ν_S(CCC) + δ(OH)	1333 (604, 184)	$\gamma(HN^+) + \nu$(ring)
1262 (1010, 151)	δ(OH) + δ_{AS}(CH) + $\delta(CH)_{PY}$	1308 (161, 42)	$\gamma(HN^+) + \delta_{AS}$(CH)
1191 (317, 16)	δ_{AS}(CH) + δ(OH)	1287 (2752, 293)	$\delta(HN^+) + \delta(CNC)_{PY}$
1159 (478, 218)	ν(CN) + δ_S(CH) + δ(OH)	1232 (2172, 87)	$\delta_S(CH)_{PY} + \nu(C-CH_3) + \delta(HN^+)$
		968 (1421, 109)	$\delta_{AS}(ring)_{PY} + \delta_{AS}(CH) + \nu_{AS}$(OHN)[d]
		791 (518, *10*)	ν_{AS}(OHN) + $\delta_{AS}(ring)_{PY}$
		777 (654, 26)	ν_{AS}(OHN) + ν(CCl)
		581 (1113, 18)	ν_{AS}(OHN)
		522 (679, 18)	$\delta_{AS}(ring)_{PY} + \nu_{AS}$(OHN)

[a] Vibrations having relative IR intensities less than 0.05 are not reported. [b] The IR intensities and Raman scattering activities are given in parentheses. [c] ν, δ, and γ denote stretching and in-plane and out-of-plane bending vibrations, respectively; index "PY" denotes the intramolecular vibrations of the pyridine molecule. [d] Schematic representations of normal coordinates for the ν_1 and ν_{AS}(OHN) vibrations of the PT state of the Py−Ph complex are given in Figure 2.

and Py−BZA, there is only one minimum on the potential energy surface that corresponds to the HB state. Selected geometrical parameters and the harmonic frequency of the OH stretching vibration associated with the HB state are collected in Table 2. An increase of the dielectric permittivity of the media results in a gradual lengthening of the O−H distance and shortening of the H···N distance that in total causes a contraction of the O···N distance. Since geometrical and spectral features of the HB state are not the main interest here, the corresponded numerical values are given in the Supporting Information to this paper: Tables S3 and S4. In the main text we are referencing to only case $\varepsilon = 4.9$ (chloroform), Table 2. For both complexes there is only one band in the 3000−1800 cm^{-1} frequency region associated with the OH stretching vibration. As a result of geometrical changes caused by the increase of ε from 1 to 4.9, the harmonic frequency of the OH stretching vibration decreases from about 3000 to 2600 cm^{-1} for Py−Ph and from about 2500 to 2300 cm^{-1} for Py−BZA (Table 2). This trend is in agreement with experiment data.[23,30] This is the most intense IR band for both complexes, Tables 3 and 4. The decrease of the frequency of the OH stretching vibration is followed by an increase of the IR intensity of this band, Figure 1 and Tables S3 and S4 (Supporting Information). According to our computations, the maximum value of the IR intensity of the OH stretching vibration is close to 6×10^3 kM/mol. It is in reasonable agreement with the values of about 5×10^3 kM/mol, experimentally obtained for the strongest H-bonds.[17]

Both complexes do not exhibit any IR-band of a remarkable intensity below 1100 cm^{-1}. Groups of intensive bands located in the 1600−1100 cm^{-1} (Py−Ph) and 1800−1300 cm^{-1} (Py−BZA) frequency regions are associated with phenol, Table 3, and carboxylic acid, Table 4, vibrations, respectively. The numerical values are similar to the ones observed experimentally for phenols and carboxylic acids.[58,59] Thus, H-bonding does not affect remarkably the spectral properties of the HB state below 1800 cm^{-1} in both complexes.

Structure and Vibrational Spectra of the PT State. According to the B3LYP-PCM computations of Py−Ph and Py−BZA, the PT state appears as a local minimum on the potential (free) energy surface at $\varepsilon > 4$ (Tables S3 and S4, Supporting Information). This estimation agrees with the available experimental data.[23,30] Proton transfer results in strong changes of the geometry of the O···H···N fragments and the lengths of the adjacent bonds (Table 2). As a result, the IR spectra of the HB and PT states differ strongly (Tables 3 and 4). We remember that in the HB state for both the Py−Ph and the Py−BZA complexes there is only one band in the 3000−1800 cm^{-1} region, which is associated with the OH stretching vibration. The frequency of this vibration decreases

TABLE 4: Harmonic Frequencies (Freq, cm^{-1}), IR Intensities[a] (*I*, kM/mol), and Raman Scattering Activities (*R*, A^4/amu) of Vibrations Involving Large Displacements of the Bridging Proton Computed for the HB and the PT States of the Py−BZA Complex at $\varepsilon = 4.9$ (Chloroform)

HB state		PT state	
freq (*I*, *R*)[b]	assignment[c]	freq (*I*, *R*)	assignment
2289 (6166, 823)	ν(OH)	1819 (2083, 45)	$\nu(HN^+)$
1763 (450, 179)	$\nu_{AS}(CO_2) + \delta$(OH)	1748 (227, 20)	$\delta(HN^+) + \nu$(CN)
1331 (913, 7)	δ(OH) + $\nu_S(CO_2)$	1681 (351, 39)	$\delta(HN^+) + \nu(CCC)_{PY}$
		1553 (957, 21)	$\nu(HN^+) + \nu_S(CO_2^-)$
		1371 (876, 56)	$\gamma(HN^+) + \nu_S(CO_2^-)$
		1344 (227, 20)	$\gamma(HN^+) + \delta_S(CCC)_{PY}$
		1296 (1796, 27)	$\gamma(HN^+)$
		980 (230, 30)	$\delta_S(CCC)_{PY} + \nu(HN^+)$
		898 (1189, 49)	$\nu(HN^+) + \delta(CNC)_{PY}$
		496 (495, 12)	$\delta_{AS}(CCC)_{PY} + \nu(HN^+)$

[a] The IR intensity is given in parentheses; vibrations having relative IR intensities less than 0.05 are not reported. [b] The IR intensities and Raman scattering activities are given in parentheses. [c] ν, δ, and γ denote stretching and in-plane and out-of-plane bending vibrations, respectively; index "PY" denotes the intramolecular vibrations of the pyridine molecule.

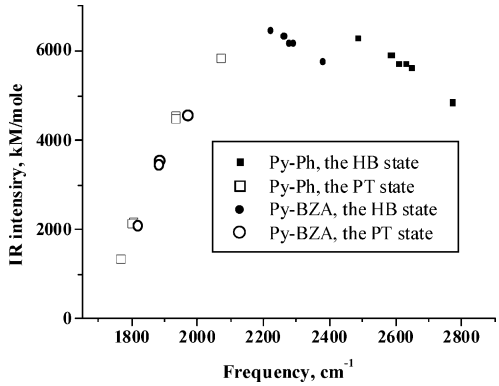

Figure 1. Dependence of the IR intensity on the frequency of the OH stretching vibration (black boxes) and the mixed vibration of the bridging proton (empty boxes) of the Py−Ph complex and the OH (black circles) and the HN^+ stretching vibrations (empty circles) of the Py−BZA complex computed at different values of the dielectric permittivity of the media ε varying from 1 to 36.6.

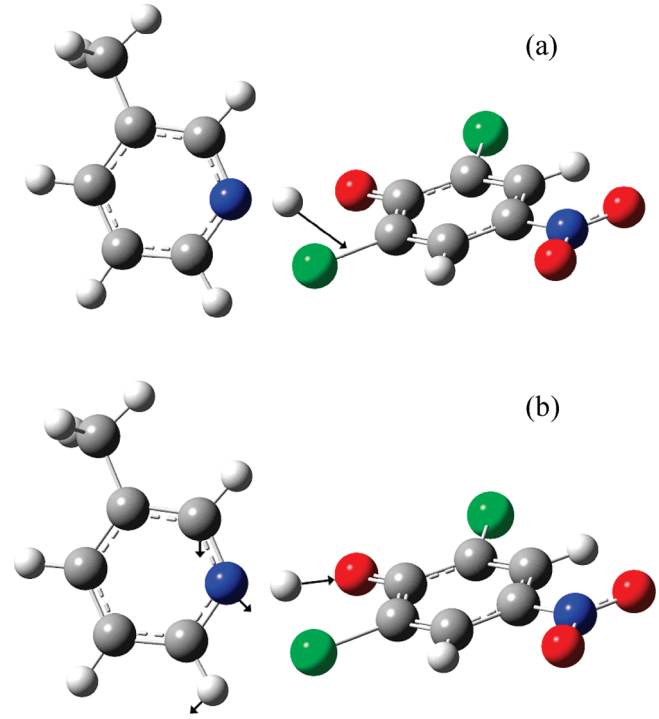

Figure 2. Schematic representation of the normal coordinates of the PT state of the Py−Ph complex: the mixed vibration of the bridging proton, ν_1 (upper panel); the asymmetric stretching vibrations of the $O^-\cdots HN^+$ fragment, ν_{AS}(OHN) (lower panel). Arrows indicate directions of relative atom displacements. The red, yellow, blue, large gray, and small gray balls denote oxygen, chlorine, nitrogen, carbon, and hydrogen atoms, respectively.

upon an increase of the dielectric permittivity of the aprotic solvent that is upon a lengthening of the O···H distance and the associated contraction of the O···N distance. In agreement with experimental data,[30] the PT state of both complexes is characterized by a band in the ~2100−1700 cm^{-1} region. The frequency of this vibration increases upon a shortening of the H···N distance and the associated lengthening of the O···N distance, Tables S3 and S4 (Supporting Information). In contrast to the OH stretching in the HB state, the IR intensity of the considered band in the PT state increases with an increase of its frequency (Figure 1). This trend indicates that the increase of the IR intensity follows an increase of the dipole moment of the complexes. However, the nature of the band in the PT state is different for Py−BZA and Py−Ph. In Py−BZA it is a stretching vibration of the HN^+ group, while in Py−Ph it is the mixed vibration of the bridging proton, ν_1 (Figure 2). This vibration cannot be assigned as the stretching or bending vibrations of the HN^+ group or the asymmetric stretching vibrations of the $O^-\cdots HN^+$ fragment. Besides that, both complexes exhibit in the PT state an intense IR band near 1350 cm^{-1} associated with the out-of-plane motion of the bridging proton. This vibration was observed experimentally as well.[60]

The PT state manifests itself most noticeably in the region below 1000 cm^{-1}.[30] This is due to a strong coupling of shared proton vibrations to other vibrations, Tables 3 and 4. As a result, several IR intensive bands associated with the stretching motion of the bridging proton appear in the PT state of both complexes in the considered region. A similar situation was observed for the KH maleate crystal (see Table 1 in ref 41) characterized by a strong (short) quasi-linear intramolecular H-bond.[61]

We draw special attention to an intense IR band at 600 cm^{-1} of the Py−Ph complex in the PT state, Figure 3. This band is associated with the asymmetric stretching vibrations of the $O^-\cdots HN^+$ fragment, Figure 2b. The IR intensity of this band increases with the decrease of the O···N distance that is the IR intensity is proportional to the H-bond energy, Table S3 (Supporting Information). Remarkably, there are no other intense IR transitions near 600 cm^{-1}. Results of our computations at $\varepsilon = 4.9$ (chloroform) show that the pyridinium cation does not have any intense IR band in the considered region. A calculated

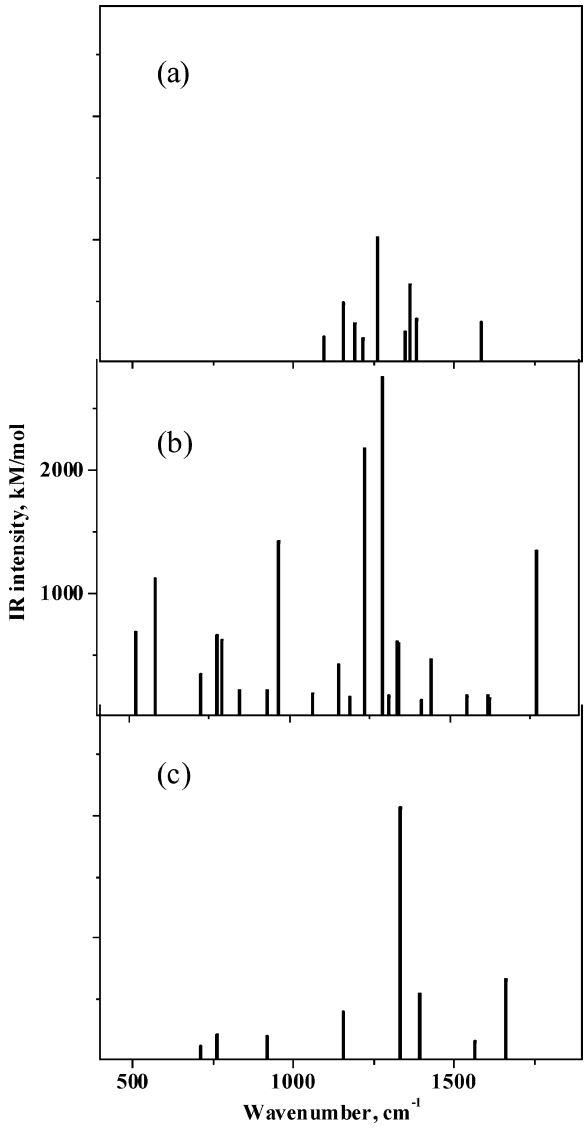

Figure 3. Computed IR spectra in the 1800−400 cm^{-1} region at ε = 4.9 (chloroform): (a) the HB state of the Py−Ph complex; (b) the PT state of the Py−Ph complex; (c) 2,6-dichloro-4-nitrophenolate ion. The height of the sticks is proportional to the relative IR intensity of the corresponding transition.

IR spectrum of 2,6-dichloro-4-nitrophenolate ion is depicted in Figure 3. The only noticeable IR transition below 1000 cm^{-1} is expected at 750 cm^{-1}, whose intensity should be about 3 times smaller as compared to the transition at 600 cm^{-1}. This observation enables us to suggest a criterion feasible to differentiate between the HB and PT states of the 1:1 complexes of phenols with pyridines in solution. We predict that the appearance of an intense band near 600 cm^{-1} in an IR spectrum of such complexes can be used as indicative of the formation of the PT state. We remember that in the crystalline form the Py−Ph complex is characterized by a short O···N distance (2.544 Å) with the bridging proton located near the nitrogen.[7] The IR spectrum of the considered complex in KBr pellet shows a relatively broad and intensive band around 570 cm^{-1}. It is worth noting that the asymmetric stretching vibration of about 550 cm^{-1} was detected for the KH maleate crystal.[41,62,63]

In the PT state of Py−BZA the CO distances of the deprotonated carboxylic group become practically equal, Table 2. As a result, instead of the carbonyl band of the CO_2H group at 1760 cm^{-1} one observes the band of the CO_2^- group around 1650 cm^{-1}, Table S4 (Supporting Information), in agreement with experimental data.[30]

Raman spectroscopy is less efficient in the identification of the HB and PT states. Our computations show that the ν(OH) vibration is characterized by a very large value of the Raman scattering activity, while the latter is negligible for the ν_1 and $\nu(HN^+)$ vibrations in the PT state of the Py−Ph and Py−BZA complexes, respectively, Tables 3 and 4. However, it can be very useful when the HB state is present in a small mole fraction.

Discussion

The obtained structures of the HB and PT states are characterized by a well-defined location of the bridging proton close to the oxygen or to the nitrogen atoms, respectively, Figure S2 and Tables S3 and S4 (Supporting Information). This observation contradicts in some ways the available experimental data for the Py−BZA type systems, which were interpreted as indicative of the formation of a quasi-symmetric H-bond at certain values of ε.[64,65] This discrepancy may be due to the neglect of the mechanical anharmonicity[43,46,47] or/and the static treatment of the media[66] in our calculations.

A family of aprotic solvents with ε varying from 2.4 (toluene) to 36.6 (acetonitrile) are considered in the present study. According to the B3LYP-PCM computations, the O···N distance in the HB and PT states of the Py−Ph complex changes monotonously (Figure S3, Supporting Information). However, the data obtained for diethyl ether and acetone do not lie on the curve. It may be caused by specific values of the parameters used in the PCM evaluation of the electrostatic and nonelectrostatic parts of the solvation energy in diethyl ether and acetone.[33]

The frequency of the OH stretching band depends on both the nature of the proton donor and the H-bond geometry of the HB state; however, it is well separated from the corresponding band of the PT state. The latter is shifted down to 2000 cm^{-1}, and its nature depends on the specific complex. In Py−BZA it is the stretching vibration of the HN^+ group. We assume that a substitution of another derivative of benzoic acid will affect the frequency of this vibration only indirectly by means of the effect on the geometry of the H-bond. In contrast, in Py−Ph it is the mixed vibration of the bridging proton. Thus, the frequency of this vibration should depend on both the geometry of the H-bond and the structure of the phenol derivative.

In some 1:1 complexes formed by phenols with pyridines[32] the IR-active band in the 2800−1800 frequency region disappears completely. A similar phenomenon is observed for the systems with strong intramolecular H-bonds of the O−H···O,[67] O−H···N,[68] and N−H···N[69] types. In the case of the KH maleate crystal, the absence of IR-active bands in the considered region is associated with an extremely shallow barrierless potential of the H-bond.[41] We can speculate that a similar situation exists in many systems with strong (short) intra- and intermolecular H-bonds.[67−69] In contrast, the appearance of widely separated bands in this frequency region is associated with a double-minimum potential.[30] An accurate computation of this potential requires the consideration of a three-dimensional free energy surface based on the bridging proton coordinate, the O···N distance, and the medium coordinate.[66] Calculation procedures accounted for the medium coordinate feasible to describe proton transfer in a polar solvent were developed. It can be done with either the molecular dynamics[70] or the continuum approximation.[71] However, both procedures are quite cumbersome and have not ever been applied for computations of the potential barrier in such big systems, as complexes of substituted pyridines with benzoic acid and phenol derivatives.

Conclusions

According to the B3LYP-PCM computations, a stable structure with proton transfer (the PT state) appears at $\varepsilon > 4$ for the 1:1 complexes of 3-methylpyridine with 2,6-dichloro-4-nitrophenol (Py−Ph) and 2,4,6-trimethylpyridine with 3,5-dinitrobenzoic acid (Py−BZA). The PT state has a distinct band that locates in the 2100−1800 cm^{-1} region. Its IR intensity decreases with the decrease of its frequency. The nature of the band is different in the Py−Ph and Py−BZA complexes. In Py−BZA it is the stretching vibration of the HN^+ group, while in Py−Ph it is the specific vibration of the bridging proton. Raman scattering activity of the OH stretching in the HB state is at least 1 order of magnitude bigger than that of any other vibration in the PT state. This feature can be helpful when the state without proton transfer is present in a small mole fraction.

A specific feature of the PT state of Py−Ph is an intense IR band near 600 cm^{-1} associated with an asymmetric stretching vibration of the $O^-\cdots HN^+$ fragment. The intensity of this band is reciprocally proportional to the O···N distance, which is proportional to the H-bond energy. The presence of this band can be used as an additional criterion of the formation of the PT state in complexes of pyridines with phenols.

Bader analysis of the electron density enables us to predict that the H-bond geometry in 1:1 crystalline complexes of pyridine with ortho-substituted phenols should be affected by noncovalent intermolecular interactions involving the ortho groups of the phenols. A proton of a nonsubstituted ortho position of phenol interacts with the nitrogen of the pyridine molecule. In contrast, a chlorine of an ortho-chloro-substituted phenol interacts with a proton in the ortho position of the pyridine molecule. The latter interaction results in a dramatic change of the dihedral angle between the two aromatic rings that leads to a contraction of the O···N distance. Thus, a selected ortho substitution can be used to control the H-bond geometry in crystalline complexes of pyridine with phenols.

Acknowledgment. This study was supported by the Russian Foundation for Basic Research (grants 08-03-00361, 08-03-00515, and 09-03-91336), the Federal Agency for Science and Innovation (Contract No. 02.740.11.0214), the Russian Ministry of Education and Science (Project RNP 2.1.1. 485) and DAAD (the scholarship program "Research stays for University Academics and Scientists"). M.V.V. thanks Prof. S. Scheiner for help in numerical computations and Drs. R. E. Asfin, V. A. Bataev, and P. M. Tolstoy for useful discussions.

Supporting Information Available: Computed values of selected geometrical parameters, the harmonic frequency of the OH stretching vibration, ν(OH), and topological characteristics of the intermolecular H-bond and noncovalent interactions of complexes of 3-methylpyridine with substituted phenols in the gas phase (Tables S1 and S2). Molecular graphs and the critical point pattern in complexes of 3-methylpyridine with substituted phenols (Figure S1). Selected geometrical parameters, the dipole moment, the relative stability of the HB and PT states of the Py−Ph and Py−BZA complexes at different values of the dielectric permittivity of the media, computed using the B3LYP-PCM approximation (Tables S3 and S4). Geometric H-bond correlation q_2 vs q_1, where q_1 and q_2 are the natural H-bond coordinates, computed for the Py−Ph complex at different values of the dielectric permittivity of the media (Figure S2). O···N distance in the HB and PT states of the Py−Ph complex as a function of solvent dielectric permittivity (Figure S3). This material is available free of charge via the Internet at http://pubs.acs.org.

References and Notes

(1) Majerz, I.; Koll, A. *Acta Crystallogr. B* **2004**, *60*, 406.
(2) Bureiko, S. F.; Golubev, N. S.; Denisov, G. S.; Kucherov, S. Yu.; Tolstoi, P. M. *Russ. J. Gen. Chem.* **2005**, *75*, 1821.
(3) Grech, E.; Kalenik, J.; Sobczyk, L. *J. Chem. Soc., Faraday Trans. I* **1979**, *75*, 1587.
(4) Szafran, M. *J. Mol. Struct.* **1996**, *381*, 39, and references therein.
(5) Steiner, T. *J. Phys. Chem. B* **1998**, *102*, 7041.
(6) Golubev, N. S.; Smirnov, S. N.; Schah-Mohammedi, P.; Shenderovich, I. G.; Denisov, G. S.; Gindin, V. A.; Limbach, H.-H. *Russ. J. Gen. Chem.* **1997**, *67*, 1150.
(7) Majerz, I.; Sawka-Dobrowolska, W.; Sobczyk, L. *J. Mol. Struct.* **1993**, *297*, 177.
(8) Golubev, N. S.; Denisov, G. S.; Smirnov, S. N.; Shchepkin, D. N.; Limbach, H.-H. *Z. Phys.Chem.* **1996**, *196*, 73.
(9) Lorente, P.; Shenderovich, I. G.; Golubev, N. S.; Denisov, G. S.; Buntkowsky, G.; Limbach, H.-H. *Magn. Reson. Chem.* **2001**, *39*, S18.
(10) Majerz, I.; Gutmann, M. J. *J. Phys. Chem. A* **2008**, *112*, 9801.
(11) Ratajczak, H.; Sobczyk, L. *J. Chem. Phys.* **1969**, *50*, 556.
(12) Sharif, S.; Fogle, E.; Toney, M. D.; Denisov, G. S.; Shenderovich, I. G.; Buntkowsky, G.; Tolstoy, P. M.; Chan Huot, M.; Limbach, H.-H. *J. Am. Chem. Soc.* **2007**, *129*, 9558.
(13) Manriquez, R.; Lopez-Dellamary, F. A.; Frydel, J.; Emmler, T.; Breitzke, H.; Buntkowsky, G.; Limbach, H.-H.; Shenderovich, I. G. *J. Phys. Chem. B* **2009**, *113*, 934.
(14) Mauder, D.; Akcakayiran, D.; Lesnichin, S. B.; Findenegg, G. H.; Shenderovich, I. G. *J. Phys. Chem. C* **2009**, *113*, 19185.
(15) Childs, S. L.; Stahly, G. P.; Park, A. *Molec. Pharmaceutics* **2007**, *4*, 323.
(16) Novak, A. *Struct. Bonding (Berlin)* **1974**, *18*, 177.
(17) Iogansen, A. V. *Spectrochim. Acta. A* **1999**, *55*, 1585.
(18) Sokolov, N. D.; Vener, M. V.; Savel'ev, V. A. *J. Mol. Struct.* **1990**, *222*, 365.
(19) Majerz, I.; Malarski, Z.; Sobczyk, L. *Chem. Phys. Lett.* **1997**, *274*, 361.
(20) Steiner, T.; Majerz, I.; Wilson, C. C. *Ang. Chem. Int. Ed.* **2001**, *40*, 2651.
(21) Cowan, J. A.; Howard, J. A. K.; McIntyre, G. J.; Lo, S. M.-F.; Williams, I. D. *Acta Crystallogr. B* **2003**, *59*, 794.
(22) Cowan, J. A.; Howard, J. A. K.; McIntyre, G. J.; Lo, S. M.-F.; Williams, I. D. *Acta Crystallogr. B* **2005**, *61*, 724.
(23) Malarski, Z.; Rospenk, M.; Sobczyk, L.; Grech, E. *J. Phys. Chem.* **1982**, *86*, 401.
(24) Shattock, T. R.; Arora, K. K.; Vishweshwar, P.; Zaworotko, M. J. *Cryst. Growth Design* **2008**, *8*, 4533.
(25) Sarma, B.; Nath, K. K.; Bhogala, B. R.; Nangia, A. *Cryst. Growth Design* **2009**, *9*, 1546.
(26) Mohamed, S.; Tocher, D. A.; Vickers, M.; Karamertzanis, P. G.; Price, S. L. *Cryst. Growth Design* **2009**, *9*, 2881.
(27) Vera, F.; Almuzara, C.; Orera, I.; Barberá, J.; Oriol, L.; Serrano, J. L.; Sierra, T. *J. Polym. Sci. Part A: Polym. Chem.* **2008**, *46*, 5528.
(28) Czerwinski, R. M.; Harris, T. K.; Massiah, M. A.; Mildvan, A. S.; Whitman, C. P. *Biochemistry* **2001**, *40*, 1984.
(29) Massiah, M. A.; Viragh, C.; Reddy, P. M.; Kovach, I. M.; Johnson, J.; Rosenberry, T. N.; Mildvan, A. S. *Biochemistry* **2001**, *40*, 5682.
(30) Johnson, S. L.; Rumon, K. A. *J. Phys. Chem.* **1965**, *69*, 74.
(31) Schmidtmann, M.; Wilson, C. C. *Cryst. Eng. Commun.* **2008**, *10*, 177.
(32) Malarski, Z.; Majerz, I.; Lis, T. *J. Mol. Struct.* **1987**, *158*, 369.
(33) Tomasi, J.; Mennucci, B.; Cammi, R. *Chem. Rev.* **2005**, *105*, 2999.
(34) Sousa, C. F.; Fernandes, P. A.; Ramos, M. J. *J. Phys. Chem. A* **2007**, *111*, 10439.
(35) Koch, W.; Holthausen, M. C. *A Chemist's guide to density functional theory*; Wiley-VCH: Weinheim:, 2001; 300 pp.
(36) Civalleri, B.; Doll, K.; Zicovich-Wilson, C. M. *J. Phys. Chem. B* **2007**, *111*, 26.
(37) Tosoni, S.; Tuma, C.; Sauer, J.; Civalleri, B.; Ugliengo, P. *J. Chem. Phys.* **2007**, *127*, 154102.
(38) Vener, M. V.; Manaev, A. V.; Egorova, A. N.; Tsirelson, V. G. *J. Phys. Chem. A* **2007**, *111*, 1155.
(39) Wieczorek, R.; Dannenberg, J. J. *J. Phys. Chem. B* **2008**, *112*, 1320.
(40) LaPointe, S. M.; Farrag, S.; Bohórquez, H. J.; Boyd, R. J. *J. Phys. Chem. B* **2009**, *113*, 10957.
(41) Vener, M. V.; Manaev, A. V.; Tsirelson, V. G. *J. Phys. Chem. A* **2008**, *112*, 13628.
(42) Valeev, E. F.; Schaefer, H. F. *J. Chem. Phys.* **1998**, *108*, 7197.
(43) Del Bene, J. E.; Jordan, M. J. T.; Gill, P. M. W.; Buckingham, A. D. *Mol. Phys.* **1997**, *92*, 429.
(44) Silvi, B.; Wieczorek, R.; Latajka, Z.; Alikhani, M. E.; Dkhissi, A.; Bouteiller, Y. *J. Chem. Phys.* **1999**, *111*, 6671.
(45) Naundorf, H.; Organero, J. A.; Douhal, A.; Kühn, O. *J. Chem. Phys.* **1999**, *110*, 11286.

(46) Balazic, K.; Stare, J.; Mavri, J. *J. Chem. Inf. Model.* **2007**, *47*, 832.
(47) Stare, J.; Panek, J.; Eckert, J.; Grdadolnik, J.; Mavri, J.; Hadzi, D. *J. Phys. Chem. A* **2008**, *112*, 1576.
(48) Frisch, M. J.; Trucks, G. W.; Schlegel, H. B.; Scuseria, G. E.; Robb, M. A.; Cheeseman, J. R.; Montgomery, J. A., Jr.; Vreven, T.; Kudin, K. N.; Burant, J. C.; Millam, J. M.; Iyengar, S. S.; Tomasi, J.; Barone, V.; Mennucci, B.; Cossi, M.; Scalmani, G.; Rega, N.; Petersson, G. A.; Nakatsuji, H.; Hada, M.; Ehara, M.; Toyota, K.; Fukuda, R.; Hasegawa, J.; Ishida, M.; Nakajima, T.; Honda, Y.; Kitao, O.; Nakai, H.; Klene, M.; Li, X.; Knox, J. E.; Hratchian, H. P.; Cross, J. B.; Bakken, V.; Adamo, C.; Jaramillo, J.; Gomperts, R.; Stratmann, R. E.; Yazyev, O.; Austin, A. J.; Cammi, R.; Pomelli, C.; Ochterski, J. W.; Ayala, P. Y.; Morokuma, K.; Voth, G. A.; Salvador, P.; Dannenberg, J. J.; Zakrzewski, V. G.; Dapprich, S.; Daniels, A. D.; Strain, M. C.; Farkas, O.; Malick, D. K.; Rabuck, A. D.; Raghavachari, K.; Foresman, J. B.; Ortiz, J. V.; Cui, Q.; Baboul, A. G.; Clifford, S.; Cioslowski, J.; Stefanov, B. B.; Liu, G.; Liashenko, A.; Piskorz, P.; Komaromi, I.; Martin, R. L.; Fox, D. J.; Keith, T.; Al-Laham, M. A.; Peng, C. Y.; Nanayakkara, A.; Challacombe, M.; Gill, P. M. W.; Johnson, B.; Chen, W.; Wong, M. W.; Gonzalez, C.; Pople, J. A. *Gaussian 03*, revision D.01; Gaussian, Inc.: Wallingford, CT, 2004.
(49) Barone, V.; Cossi, M. *J. Phys. Chem. A* **1998**, *102*, 1995.
(50) Bader, R. F. W. *Atoms in Molecules. A Quantum Theory*; Oxford University Press, New York, 1990.
(51) Bieger-Konig, W. F.; Bader, R. F. W.; Tang, T.-H. *J. Comput. Chem.* **1982**, *3*, 317.
(52) Bieger-Konig, W. F.; Schonbohm, J.; Bayles, D. *J. Comput. Chem.* **2001**, *22*, 245.
(53) Espinosa, E.; Molins, E.; Lecomte, C. *Chem. Phys. Lett.* **1998**, *285*, 170.
(54) Espinosa, E.; Molins, E. *J. Chem. Phys.* **2000**, *113*, 5686.
(55) Sobczyk, L.; Grabowski, S. J.; Krygowski, T. M. *Chem. Rev.* **2005**, *105*, 3513.
(56) Vener, M. V.; Egorova, A. N.; Fomin, D. P.; Tsirelson, V. G. *Chem. Phys. Lett.* **2007**, *440*, 279.
(57) Vener, M. V.; Egorova, A. N.; Fomin, D. P.; Tsirelson, V. G. *J. Phys. Org. Chem.* **2009**, *22*, 177.
(58) Keresztury, G.; Billes, F.; Kubinyi, M.; Sundius, T. *J. Phys. Chem. A* **1998**, *102*, 1371.
(59) Zelsmann, H. R.; Mareshal, Y. *Chem. Phys.* **1977**, *20*, 445.
(60) Hadzi, D.; Sheppard, N. *Proc. R. Soc. (London)* **1953**, *A216*, 247.
(61) Fillaux, F.; Leygue, N.; Tomkinson, J.; Cousson, A.; Paulus, W. *Chem. Phys.* **1999**, *244*, 387.
(62) Ilczyszyn, M. M.; Baran, J.; Ratajczak, H.; Barnes, A. J. *J. Mol. Struct.* **1992**, *270*, 499.
(63) Ratajczak, H.; Barnes, A. J.; Baran, J.; Yaremko, A. M.; Latajka, Z.; Dopieralski, P. *J. Mol. Struct.* **2008**, *887*, 9.
(64) Limbach, H. H.; Pietrzak, M.; Sharif, S.; Tolstoy, P. M.; Shenderovich, I. G.; Smirnov, S. N.; Golubev, N. S.; Denisov, G. S. *Chem.—Eur. J.* **2004**, *10*, 5195.
(65) Tolstoy, P. M.; Smirnov, S. N.; Shenderovich, I. G.; Golubev, N. S.; Denisov, G. S.; Limbach, H.-H. *J. Mol. Struct.* **2004**, *700*, 19.
(66) Basilevsky, M. V.; Vener, M. V. *Usp. Khim.* **2003**, *72*, 3.
(67) Filarowski, A.; Koll, A.; Karpfen, A.; Wolschann, P. *Chem. Phys.* **2004**, *297*, 323.
(68) Majewska, P.; Pajak, M.; Rospenk, M.; Filarowski, A. *J. Phys. Org. Chem.* **2009**, *22*, 130.
(69) Dijkstra, E.; Hutton, A. T.; Irving, H. M. N. H.; Nassimbeni, L. R. *Tetrahedron Lett.* **1981**, *22*, 4037.
(70) Staib, A.; Borgis, D.; Hynes, J. T. *J. Chem. Phys.* **1995**, *102*, 2487.
(71) Basilevsky, M. V.; Soudackov, A. V.; Vener, M. V. *Chem. Phys.* **1995**, *200*, 87.

JP911694R